ELSEVIER

Journal of Chromatography A, 921 (2001) 135–145

JOURNAL OF CHROMATOGRAPHY A

www.elsevier.com/locate/chroma

Modeling and analysis of the dynamic behavior of mechanisms that result in the development of inner radial humps in the concentration of a single adsorbate in the adsorbed phase of porous adsorbent particles observed in confocal scanning laser microscopy experiments: diffusional mass transfer and adsorption in the presence of an electrical double layer

A.I. Liapis[a,*], B.A. Grimes[a], K. Lacki[b], I. Neretnieks[c]

[a]*Department of Chemical Engineering and Biochemical Processing Institute, University of Missouri-Rolla, Rolla, MO 65409-1230, USA*

[b]*Amersham Pharmacia Biotech, Björkgatan 30, SE-751 84 Uppsala, Sweden*

[c]*Department of Chemical Engineering and Technology, Royal Institute of Technology, SE-100 44 Stockholm, Sweden*

Received 31 January 2001; received in revised form 20 April 2001; accepted 20 April 2001

Abstract

A theoretical model for adsorption of a single charged adsorbate that accounts for the presence of an electrical double layer in the pores of adsorbent particles is constructed and solved. The dynamic behavior of the mechanisms of the model can result in the development of inner radial humps (concentration rings) in the concentration of a single charged analyte (adsorbate) in the adsorbed phase of porous adsorbent particles. The results of the present work demonstrate the implication of the concept regarding the effect of the presence of an electrical double layer in the pores of adsorbent particles and the induced interactions between the electrostatic potential distribution and the mechanisms of mass transport of the species by diffusion, electrophoretic migration, and adsorption. Furthermore, the mechanisms of the model could explain qualitatively the development of the concentration ring (hump) observed in confocal scanning laser microscopy experiments.

Keywords: Inner radial humps; Electrical double layer; Confocal scanning laser microscopy; Porous adsorbent particles; Adsorption; Diffusional mass transfer; Electrophoretic mass transfer

1. Introduction

The kinetic and equilibrium characteristics of the adsorption of solutes onto different types of porous adsorbent particles has been studied by analyzing uptake and breakthrough curves obtained from finite bath (batch) and column experiments, respectively, in which the concentration of the adsorbate in the bulk solid phase is determined from the reduction of the concentration of the adsorbate in the bulk fluid

*Corresponding author. Tel.: +1-573-3414-416; fax: +1-314-9659-329.

0021-9673/01/$ – see front matter
PII: S0021-9673(01)00878-0

phase [1–3]. The experimental information obtained from batch and column experiments can only provide an indirect measurement of the concentration of adsorbate within the adsorbent particles. The method of confocal scanning laser microscopy has been recently shown [3–10] to provide direct experimental information for monitoring the dynamic and equilibrium behavior of the adsorption process of a solute within a single porous adsorbent particle. This direct experimental information of the behavior of the adsorbate in the adsorbent particles will increase significantly our scientific understanding with regard to the adsorption process and will enable us to characterize accurately the quantitative behavior of the intraparticle diffusional and convective mass transfer and adsorption mechanisms [1,2,11–13].

The direct experimental information obtained from the method of confocal scanning laser microscopy has shown the extremely interesting experimental result [3,7,9,10] that single component adsorption involving charged adsorbate molecules adsorbing onto the pore surface of ion-exchange adsorbent particles could have adsorbed phase concentrations, under certain conditions of ionic strength and pH, that are higher at certain positions within the particle than positions at parts of the particle closer to the particle surface or at positions closer to the particle center. This hump [3,7,9,10] in the adsorbed concentration of the adsorbate along a certain inner portion of the particle radius results in the formation of a so-called concentration ring. The indirect experimental information obtained from the finite bath or column experiments discussed above, cannot provide any information regarding the formation of an adsorbate concentration ring in the adsorbed phase of the porous adsorbent particles. It is very important to mention here that adsorption models that neglect the presence of an electrical double layer in the pores of ion-exchange adsorbent particles and consider adsorption of a single charged component where intraparticle mass transfer occurs by pore [1,2] and/or surface [2] diffusion, cannot provide an adsorbate concentration ring in the adsorbed phase of the porous adsorbent particles; such models only provide a monotonic decrease in the concentration of the adsorbate in the adsorbed phase from the surface of the particle to the center of the particle.

It has been observed [7,9,10] that the appearance of the adsorbate concentration humps in the adsorbed phase depends on the values of the pH and ionic strength of the solution for a given charged adsorbate (protein) and a given charged adsorbent particle. These observations [7,9,10] suggest to us that electrical double layer interactions could be involved as intraparticle mass transfer of the charged species (cation and anion of the electrolyte as well as the adsorbate) and adsorption of the adsorbate occur. In this work, a mathematical model that accounts for the presence of an electrical double layer in the pores of adsorbent particles is presented, and the mechanisms of the model could explain qualititatively the development of the concentration ring in the adsorbed phase of the adsorbate within the adsorbent particles.

2. Formulation of mathematical model

The intraparticle pore surfaces of the porous adsorbent particles are considered to bear a local fixed surface charge density, δ, and the adsorbate (component 3) as well as the cations (component 1) and anions (component 2) of the buffer electrolyte bear formal charges in the intraparticle pore fluid. Thus, there is an electrical double layer in contact with the surface of the intraparticle pores. The expression for determining the electrostatic potential, Φ, along the radial direction, ρ, of a cylindrical pore of radius ρ_{pore} at any radial position, r, along the particle radius, r_p, is given by the Poisson–Boltzmann equation whose form [14] is as follows:

$$\frac{d^2\Phi}{d\rho^2}+\frac{1}{\rho}\cdot\frac{d\Phi}{d\rho}=-\frac{N_0 e}{\epsilon\epsilon_0}\cdot\left[z_1 C_{p1,ec}(t,r)\exp\left(-\frac{z_1 e}{kT}\Phi\right)+z_2 C_{p2,ec}(t,r)\exp\left(-\frac{z_2 e}{kT}\Phi\right)+z_3 C_{p3,ec}(t,r)\exp\left(-\frac{z_3 e}{kT}\Phi\right)\right] \quad (1)$$

In Eq. (1), ϵ and ϵ_0 denote the dielectric constant and the permittivity of free space, respectively; N_0 is Avogadro's number, e is the charge of one electron,

k is the Boltzmann constant, T represents the absolute temperature, z_i ($i=1, 2, 3$) denotes the charge number of component i, and $C_{pi,ec}$ ($i=1, 2, 3$) denotes the concentration of component i in the electroneutral core region of the intraparticle pore (electrolyte concentrations and values of ρ_{pore} employed in this work and encountered most often in practice provide no overlap of the double layer in the intraparticle pores). Eq. (1) accounts for the explicit variation of the electrostatic potential along ρ and for the implicit variation of the electrostatic potential along r in the non-electroneutral region of the pore fluid, as adsorption of adsorbate occurs on the surface of the pore. It should be noted here that the adsorption process could also induce an explicit variation in the magnitude of the electrostatic potential along r in the non-electroneutral region of the pore fluid [15]; the effect of the possible explicit variation in the electrostatic potential along r will be reported in future work. Furthermore, it can be shown from the continuity and momentum balance equations for the pore fluid that the volumetric flowrate at any cross-section of the pore is equal to zero [15] and, thus, the convective velocity of the pore fluid in the pore is equal to zero [15]; in this work, the convective velocity of the pore fluid was taken to be equal to zero.

The boundary conditions for Eq. (1) are given by Eqs. (2) and (3):

$$\text{at } \rho = 0, \left.\frac{d\Phi}{d\rho}\right|_{\rho=0} = 0 \tag{2}$$

$$\text{at } \rho = \rho_{pore}, \left.\frac{d\Phi}{d\rho}\right|_{\rho=\rho_{pore}} = \frac{\delta}{\epsilon\epsilon_0} = \frac{\delta_0}{\epsilon\epsilon_0} + \frac{z_3 N_0 e}{\epsilon\epsilon_0} \cdot \frac{C_{S3}}{\xi} \tag{3}$$

where δ_0 represents the fixed charge density at the surface of the intraparticle pore when no adsorption has occurred, ξ is the particle phase ratio, and C_{S3} represents the concentration of the adsorbate in the adsorbed phase. The value of C_{S3} is obtained from the adsorption isotherm. In this work, the Langmuir adsorption isotherm is considered for single component adsorption and its form is given by Eq. (4):

$$C_{S3} = \frac{C_T K C_{p3}(t,r,\rho=\rho_{pore})}{\left[1 + K C_{p3}(t,r,\rho=\rho_{pore})\right]} \tag{4}$$

where

$$C_{p3}(t,r,\rho=\rho_{pore}) = C_{p3,ec}(t,r) \cdot \left[\exp\left(-\frac{z_3 e}{kT}\cdot\Phi(\rho=\rho_{pore})\right)\right] \tag{5}$$

In Eqs. (4) and (5), K denotes the equilibrium adsorption constant, C_T represents the maximum concentration of adsorbate in the adsorbed phase when all accessible adsorption sites are utilized, $C_{p3}(t,r,\rho=\rho_{pore})$ denotes the concentration of the adsorbate in the fluid layer immediately adjacent to the surface of the pore at time t and radial position r in the particle, and $C_{p3,ec}(t,r)$ is the concentration of the adsorbate in the electroneutral core region of the pore fluid [14]. Eq. (5) is obtained from the Boltzmann expression [14] and the exponential term $\{\exp[-(z_3 e/kT)\Phi(\rho=\rho_{pore})]\}$ multiplies the value of $C_{p3,ec}(t,r)$ in order to account for the increased concentration of the adsorbate in the electrical double layer. It is worth noting here that the value of $\Phi(\rho=\rho_{pore})$ in Eq. (5) represents the value of the zeta potential, ζ_w, at the surface of the pores; the value of $\Phi(\rho=\rho_{pore})$ changes as the concentration, C_{S3}, of the adsorbate in the adsorbed phase changes. It is important to mention here that the magnitudes of δ_0 and ζ_w depend on the values of the pH and ionic strength of the solution [15,16]; also the charge number, z_3, of the adsorbate (protein) depends on the value of the pH of the solution [16]. By combining Eqs. (4) and (5), the following expression for the Langmuir adsorption isotherm is obtained:

$$C_{S3} = \frac{C_T K C_{p3,ec}(t,r)\cdot\left[\exp\left(-\frac{z_3 e}{kT}\cdot\Phi(\rho=\rho_{pore})\right)\right]}{\left\{1 + K C_{p3,ec}(t,r)\cdot\left[\exp\left(-\frac{z_3 e}{kT}\cdot\Phi(\rho=\rho_{pore})\right)\right]\right\}} \tag{6}$$

It is worth noting here that if the adsorbate had no charge ($z_3=0$) and/or if the value of the electrostatic potential at the surface of the pore is zero [$\Phi(\rho=\rho_{pore})=0$], then the magnitude of the exponential term $\{\exp[-(z_3 e/kT)\Phi(\rho=\rho_{pore})]\}$ in Eqs. (5) and (6) would be equal to one. Furthermore, the values of the concentrations [$C_{pi}(t,r,\rho)$, $i=1, 2, 3$] of the

species along the directions r and ρ can be obtained for different times t from the Boltzmann expression [13] given by Eq. (7):

$$C_{pi}(t,r,\rho) = C_{pi,ec}(t,r)\cdot\left[\exp\left(-\frac{z_i e}{kT}\cdot\Phi(\rho)\right)\right], i = 1, 2, 3 \quad (7)$$

where $\Phi(\rho)$ is obtained from the solution of Eq. (1). In this work, the effective pore diffusion coefficient of species i ($i=1$, 2, 3) along the radial direction ρ of the pore was considered to be independent of ρ and equal to the effective pore diffusion coefficient of species i ($i=1$, 2, 3) along the radial direction r of the particle [14].

The transport of cations, anions, and adsorbate in the electroneutral core region of the pore fluid in the adsorbent particles is considered to occur by pore diffusion. The differential mass balances for the cation, anion, and adsorbate in the electroneutral core region of the pore fluid in the pores of the porous adsorbent particles are given by Eqs. (8)–(10):

$$\frac{\partial(\epsilon_p C_{p1,ec})}{\partial t} = \frac{1}{r^\alpha}\cdot\left[\sum_{j=1}^{3}\frac{\partial}{\partial r}\left(r^\alpha \epsilon_p D_{p1j}\cdot\frac{\partial C_{pj,ec}}{\partial r}\right)\right] + R_{p1} \quad (8)$$

$$\frac{\partial(\epsilon_p C_{p2,ec})}{\partial t} = \frac{1}{r^\alpha}\cdot\left[\sum_{j=1}^{3}\frac{\partial}{\partial r}\left(r^\alpha \epsilon_p D_{p2j}\cdot\frac{\partial C_{pj,ec}}{\partial r}\right)\right] + R_{p2} \quad (9)$$

$$\frac{\partial(\epsilon_p C_{p3,ec})}{\partial t} + (1-\epsilon_p)\cdot\left(\frac{\partial C_{S3}}{\partial C_{p3,ec}}\right)\cdot\frac{\partial C_{p3,ec}}{\partial t} = \frac{1}{r^\alpha}\cdot\left[\sum_{j=1}^{3}\frac{\partial}{\partial r}\left(r^\alpha \epsilon_p D_{p3j}\cdot\frac{\partial C_{pj,ec}}{\partial r}\right)\right] + R_{p3} \quad (10)$$

where t is the time, r is the radial distance in the adsorbent particle, ϵ_p denotes the porosity of the adsorbent particle, D_{pij} ($i=1$, 2, 3 and $j=1$, 2, 3) represent the effective pore diffusion coefficients of the ternary mixture (D_{p12}, D_{p13}, D_{p21}, D_{p23}, D_{p31}, and D_{p32} are the effective pore cross-diffusion coefficients while D_{p11}, D_{p22}, and D_{p33} denote the effective pore diagonal diffusion coefficients in the matrix of the effective pore diffusion coefficients of the ternary mixture), and R_{pi} ($i=1$, 2, 3) is the molar rate of production of species i per unit volume. A dilute binary electrolyte [16] is considered in the systems studied in this work and, thus [14], $R_{p1}=R_{p2}=0$, while the molar rate of production per unit volume of the adsorbate, R_{p3}, is equal to zero. Furthermore, for dilute mixtures it has been the practice to assume the vanishing [17,18] of the effective pore cross-diffusion coefficients (off-diagonal terms of the effective pore diffusivity matrix) without having an estimate of the values of these coefficients. It has been shown [17,18] that by setting the effective pore cross-diffusion coefficients equal to zero the resulting diffusion equations of the mathematical model are not self consistent. Liapis and Litchfield [19] studied the terms of the effective pore diffusivity matrix of dilute multicomponent adsorption systems involving uncharged solutes and found that the values of the off-diagonal effective pore diffusion coefficients were about two-orders of magnitude smaller than the values of the diagonal terms of the effective pore diffusivity matrix. Their results [19] showed that the usual practice of setting the off-diagonal terms of the effective pore diffusivity matrix equal to zero when the multicomponent systems are dilute, may not contribute a significant error in the model predictions. While it could be possible that in dilute multicomponent mixtures involving charged species the contribution of the off-diagonal terms of the effective pore diffusivity matrix might not provide an insignificant error in model predictions, in this work the off-diagonal terms of the effective pore diffusivity matrix were considered to be very much smaller than the diagonal terms and were set equal to zero ($D_{p12}=D_{p13}=D_{p21}=D_{p23}=D_{p31}=D_{p32}=0$). By (i) setting the off-diagonal terms of the effective pore diffusivity matrix equal to zero, (ii) representing the diagonal terms D_{p11}, D_{p22}, and D_{p33} by D_{p1}, D_{p2}, and D_{p3}, respectively, and (iii) setting $R_{p1}=R_{p2}=R_{p3}=0$ for the reasons discussed above, Eqs. (8)–(10) become as follows:

$$\frac{\partial(\epsilon_p C_{p1,ec})}{\partial t} = \frac{1}{r^\alpha}\cdot\frac{\partial}{\partial r}\left(r^\alpha \epsilon_p D_{p1}\cdot\frac{\partial C_{p1,ec}}{\partial r}\right) \quad (11)$$

$$\frac{\partial(\epsilon_p C_{p2,ec})}{\partial t} = \frac{1}{r^\alpha}\cdot\frac{\partial}{\partial r}\left(r^\alpha \epsilon_p D_{p2}\cdot\frac{\partial C_{p2,ec}}{\partial r}\right) \quad (12)$$

$$\frac{\partial(\epsilon_p C_{p3,ec})}{\partial t} + (1-\epsilon_p)\cdot\left(\frac{\partial C_{S3}}{\partial C_{p3,ec}}\right)\cdot\frac{\partial C_{p3,ec}}{\partial t} = \frac{1}{r^\alpha}\cdot\frac{\partial}{\partial r}\left(r^\alpha \epsilon_p D_{p3}\cdot\frac{\partial C_{p3,ec}}{\partial r}\right) \quad (13)$$

It should be noted here that the effects of (i) the off-diagonal terms of the effective pore diffusivity matrix, (ii) the restricted pore diffusion [12,20–22], and (iii) the possible electrophoretic migration that could occur due to the explicit variation of the electrostatic potential along r (the electrophoretic migration due to the explicit variation of the electrostatic potential along ρ and the implicit variation of the electrostatic potential along r have been accounted for in this work, as discussed in the paragraph following Eq. (1)), should be considered as being lumped in the magnitudes of the effective pore diffusion coefficients D_{p1}, D_{p2}, and D_{p3}.

Eqs. (11)–(13) can be used for particles having geometry of slab, cylinder, or sphere by putting $\alpha=0$, 1, 2, respectively. The initial and boundary conditions of Eqs. (11)–(13) are:

$$\text{at } t=0,\ C_{p1,ec}=C_{+\infty},\ \text{for } 0\le r\le r_p \quad (14)$$

$$\text{at } t=0,\ C_{p2,ec}=C_{-\infty},\ \text{for } 0\le r\le r_p \quad (15)$$

$$\text{at } t=0,\ C_{p3,ec}=0,\ \text{for } 0\le r\le r_p \quad (16)$$

$$\text{at } r=0,\ \left.\frac{\partial C_{pi,ec}}{\partial r}\right|_{r=0}=0,\ \text{for } t>0,\ i=1,2,3 \quad (17)$$

$$\text{at } r=r_p,\ \epsilon_p D_{pi}\cdot\left.\frac{\partial C_{pi,ec}}{\partial r}\right|_{r=r_p} = K_{fi}\cdot\left[C_{di}(t)-C_{pi,ec}(t,r=r_p)\right],\ \text{for } t>0,\ i=1,2,3 \quad (18)$$

In Eqs. (14)–(18), $C_{+\infty}$ and $C_{-\infty}$ represent the concentrations of the cations and anions, respectively, for $t\le 0$, r_p is the particle radius, K_{fi} ($i=1$, 2, 3) denotes the film mass transfer coefficient of component i, and $C_{di}(t)$ ($i=1$, 2, 3) is the concentration of component i in the finite bath. In the electroneutral core region of the fluid in the pores of the adsorbent particles, the electroneutrality condition requires that:

$$z_1 C_{p1,ec} + z_2 C_{p2,ec} + z_3 C_{p3,ec} = 0 \quad (19)$$

Eq. (19) was used in this work to eliminate [14] Eq. (12). Furthermore, the condition of electroneutrality was also employed in the boundary conditions given by Eqs. (17) and (18); for the concentrations of the species in the finite bath, the electroneutrality condition gives:

$$z_1 C_{d1} + z_2 C_{d2} + z_3 C_{d3} = 0 \quad (20)$$

The porous adsorbent particles are suspended in the liquid of the finite bath so that the liquid has free access, and the bulk concentration of the cations and anions of the electrolyte as well as the bulk concentration of the adsorbate are taken to be uniform throughout the bath except in a thin film (film mass transfer resistance) of liquid surrounding each particle [1,2]. A differential mass balance for the cations, anions, and the adsorbate in the liquid phase of the finite bath gives:

$$\frac{dC_{di}(t)}{dt} = \frac{(1-\epsilon_b)}{\epsilon_b}\cdot\left(\frac{\alpha+1}{r_p}\right)\cdot K_{fi}\cdot\left[C_{pi,ec}(t,r=r_p)-C_{di}(t)\right]+R_{di},\quad \text{for } i=1,2,3 \quad (21)$$

where ϵ_b denotes the void fraction in the bath, and R_{di} represents the molar rate of production of species i per unit volume of the finite bath; for the reasons discussed for R_{pi} ($i=1$, 2, 3) above, $R_{d1}=R_{d2}=R_{d3}=0$. The initial conditions of Eq. (21) are:

$$\text{at } t=0,\ C_{d1} = -\frac{z_2}{z_1}\cdot C_{-\infty} - \frac{z_3}{z_1}\cdot C^0_{d3} \quad (22)$$

$$\text{at } t=0,\ C_{d2}=C_{-\infty} \quad (23)$$

$$\text{at } t=0,\ C_{d3}=C^0_{d3} \quad (24)$$

Eq. (22) is obtained from the condition of electroneutrality [14] in the bath fluid (Eq. (20)). By employing the condition of electroneutrality ($z_1C_{d1}+z_2C_{d2}+z_3C_{d3}=0$) in Eq. (21) for species 2 (the anion), the differential mass balance equation (Eq. (21) with $i=2$) for the anion is eliminated [14]. It is worth mentioning here that the fluid phase of the finite bath plays a very important role as a source or sink for the cations, anions, and adsorbate, when the

cations, anions and adsorbate correspondingly enter in or exit from the pore fluid of the particles as the adsorption process is taking place.

The equations of the mathematical model presented above are coupled and were solved simultaneously by the numerical method of orthogonal collocation on finite elements [23,24]. The details of the numerical solution of these equations are reported in Ref. [15].

3. Results and discussion

The theoretical results describing the adsorption of a positively charged adsorbate with $z_3=1$ onto the negatively charged ($\delta_0<0$) surface of the pores of spherical adsorbent particles are presented and discussed in this section. The aqueous system is taken to be isothermal with $T=293.15$ K, the value of the dielectric constant, ϵ, of the solution is taken to be equal to 80.1, and the value of the permittivity of free space, ϵ_0 is equal to $8.85\cdot10^{-12}$ $C^2/(N\ m^2)$. The values of the initial concentrations $C_{+\infty}$ and $C_{-\infty}$ of the cations and anions, respectively, of a 1:1 ($z_1=-z_2=1$) electrolyte in the pores of the adsorbent particles are both taken to be equal to 50.0 m*M*, while the value of the initial concentration, C^0_{d3}, of the positively charged adsorbate ($z_3=1$) in the finite bath is taken to be equal to 0.025 m*M*. The radius of the particles, r_p, is taken to be equal to 50 μm, the value of the average radius of the intraparticle pores, ρ_{pore}, is considered to be equal to 150 Å, the charge density, δ_0, on the surface of the intraparticle pores before adsorption occurs is taken to be equal to -0.050 C/m^2, while the phase ratio, ξ, of the particles was considered to be equal to $2.0\cdot10^8$ m^{-1}. The values of ϵ_b, ϵ_p, K, and C_T were taken to be equal to 0.900, 0.490, 2.0 mM^{-1}, and 0.50 m*M*, respectively. The electrolyte was taken to be sodium acetate and the free molecular diffusivities, $D_{mf,i}$ ($i=1, 2, 3$), of the cation, anion, and adsorbate are $1.96\cdot10^{-9}$ m^2/s, $1.09\cdot10^{-9}$ m^2/s, and $1.00\cdot10^{-11}$ m^2/s, respectively. The values of the film mass transfer coefficients K_{f1}, K_{f2}, and K_{f3} were taken to be equal to $9.99\cdot10^{-5}$ m/s, $6.29\cdot10^{-5}$ m/s, and $2.00\cdot10^{-6}$ m/s, respectively, and were estimated from the expression given on p. 440 of Ref. [25]. The values of the effective pore diffusion coefficients D_{p1}, D_{p2}, and D_{p3} were taken to be equal to $2.59\cdot10^{-11}$ m^2/s, $2.58\cdot10^{-12}$ m^2/s, and $2.45\cdot10^{-12}$ m^2/s, respectively. For these values of the effective pore diffusion coefficients, the adsorption process of the adsorbate provided inner radial concentration humps for the given values of δ_0, ρ_{pore}, z_1, z_2, z_3, ϵ, ϵ_b, ϵ_p, K, C_T, ξ, $C_{+\infty}$, $C_{-\infty}$, C^0_{d3}, r_p, and T. It is very important to note here that if the double layer in the pores is not considered, then there are no inner radial adsorbate concentration humps for any combination of D_{p1}, D_{p2}, and D_{p3}, including for those reported above. It appears to be imperative that one should consider the double layer in the pores in order to generate inner radial adsorbate concentration humps. Furthermore, the fact that the values of D_{p1}, D_{p2}, and D_{p3} have to be significantly lower than the values of their corresponding free molecular diffusivities, indicates that mechanisms (i)–(iii) in the paragraph immediately following Eq. (13) could be playing an important role in the intraparticle multicomponent interactive mass transport processes which, in the presence of a double layer in the pores, can provide conditions for adsorbate entrapment and accumulation in the pore fluid at inner radial positions that can result in inner radial adsorbate concentration humps in the adsorbed phase. Also, the value of the effective pore diffusion coefficient, D_{p2}, of the anion is very close to the magnitude of the effective pore diffusion coefficient, D_{p3}, of the adsorbate because the effective diffusional velocity [12] of the anion in the pore fluid has to be similar to the effective diffusional velocity [12] of the adsorbate (the adsorbate is positively charged) in the pore fluid in order to entrap both positively and negatively charged species in the adsorption zone; this produces, in conjunction with the effect of the electrostatic potential, entrapment and accumulation of the charged species in the adsorption zone (generation of inner radial adsorbate concentration humps in the adsorbed phase).

In Figs. 1–7 the profiles of $C_{p1,ec}$, $C_{p2,ec}$, $C_{p3,ec}$, C_{S3}, δ, $\Phi(\rho=\rho_{pore})$, and $\exp[-(z_3e/kT)\Phi(\rho=\rho_{pore})]$ along the dimensionless radius, r/r_p, of the particle are, respectively, presented at five different times t_1, t_2, t_3, t_4, and t_5. At time $t_1=90$ s the adsorbate has not penetrated far into the particle; at time $t_2=240$ s the adsorbate has penetrated into the

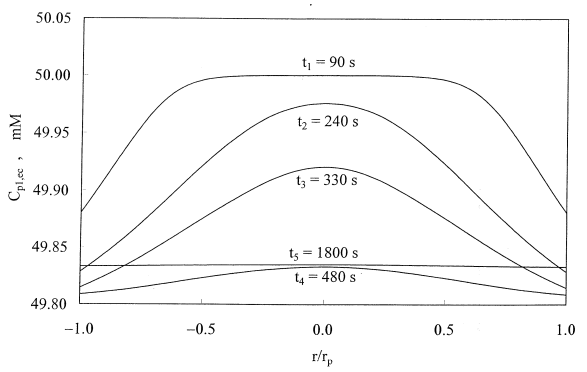

Fig. 1. Radial profile of the concentration, $C_{p1,ec}$, of the cations in the electroneutral core region of the fluid in the pores of the adsorbent particles at different times; $t_1=90$ s, $t_2=240$ s, $t_3=330$ s, $t_4=480$ s, and $t_5=1800$ s.

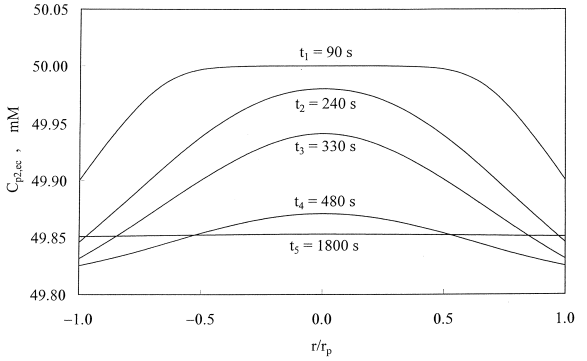

Fig. 2. Radial profile of the concentration, $C_{p2,ec}$, of the anions in the electroneutral core region of the fluid in the pores of the adsorbent particles at different times; $t_1=90$ s, $t_2=240$ s, $t_3=330$ s, $t_4=480$ s, and $t_5=1800$ s.

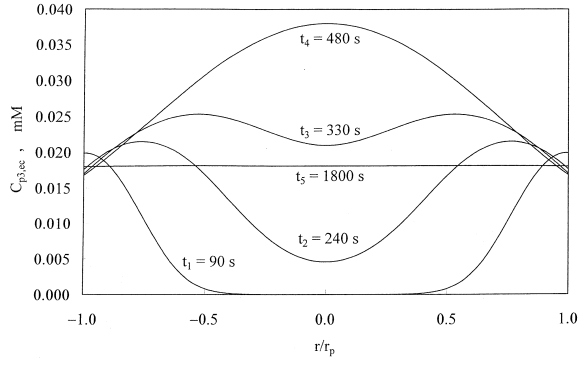

Fig. 3. Radial profile of the concentration, $C_{p3,ec}$, of the analyte (adsorbate) in the electroneutral core region of the fluid in the pores of the adsorbent particles at different times; $t_1=90$ s, $t_2=240$ s, $t_3=330$ s, $t_4=480$ s, and $t_5=1800$ s.

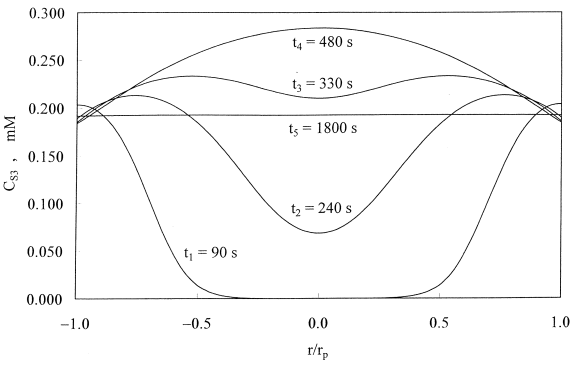

Fig. 4. Radial profile of the concentration, C_{S3}, of the analyte (adsorbate) in the adsorbed phase of the adsorbent particles at different times; $t_1=90$ s, $t_2=240$ s, $t_3=330$ s, $t_4=480$ s, and $t_5=1800$ s.

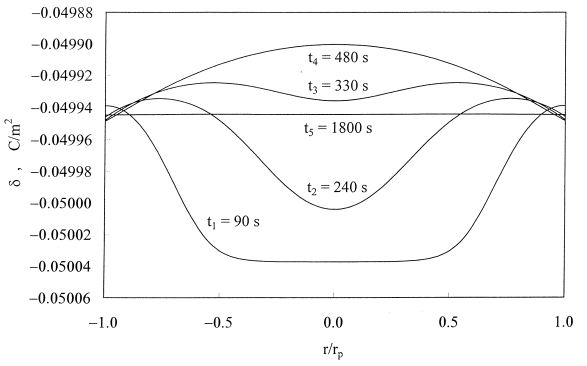

Fig. 5. Radial profile of the charge density, δ, at the surface of the pores of the adsorbent particles at different times; $t_1=90$ s, $t_2=240$ s, $t_3=330$ s, $t_4=480$ s, and $t_5=1800$ s.

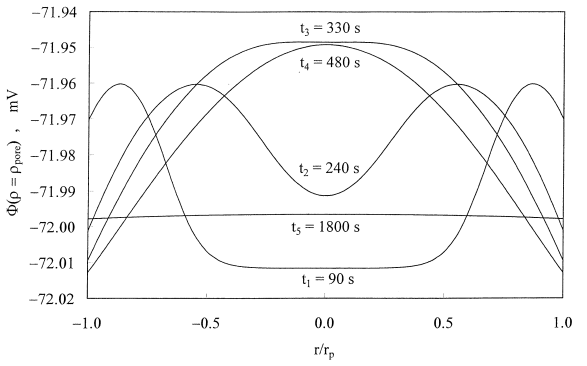

Fig. 6. Radial profile of the electrostatic potential, Φ, evaluated at the surface ($\rho=\rho_{pore}$) of the pores of the adsorbent particles at different times; $t_1=90$ s, $t_2=240$ s, $t_3=330$ s, $t_4=480$ s, and $t_5=1800$ s.

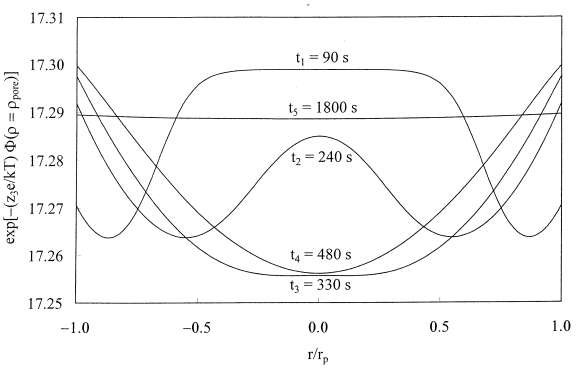

Fig. 7. Radial profile of the exponential term, $\exp[-(z_3e/kT)\Phi(\rho=\rho_{pore})]$, employed in Eqs. (5) and (6) at different times; $t_1=90$ s, $t_2=240$ s, $t_3=330$ s, $t_4=480$ s, and $t_5=1800$ s.

center of the particle ($r/r_p=0$); at time $t_3=330$ s the profile of the concentration of the adsorbate in the pore fluid, $C_{p3,ec}$, and in the adsorbed phase, C_{S3}, is approaching a maximum at the center of the particle ($r/r_p=0$), at time $t_4=480$ s the profile of the concentration of the adsorbate in the pore fluid, $C_{p3,ec}$, and in the adsorbed phase, C_{S3}, has reached a maximum at the center of the particle ($r/r_p=0$), and at time $t_5=1800$ s the equilibrium condition of the system has been established. The results shown in Fig. 1 indicate that the concentration of the cations, $C_{p1,ec}$, in the electroneutral core region of the intraparticle pores decreases from the center of the particle ($r/r_p=0$) to the surface of the particle ($r/r_p=\pm1$) in order to preserve the condition of electroneutrality by providing a diffusive flux that can transport the cations from the particle into the finite bath, as more cations are removed from the electrical double layer [14] and move into the electroneutral core region in order to accommodate [14] the adsorption process of the analyte when the adsorbate molecules are present in the electrical double layer and adsorb onto the charged surface of the pores [the values of δ and $\Phi(\rho=\rho_{pore})$ both become less negative during adsorption, as Figs. 5 and 6 indicate]; therefore, the total amount of cations in the electrical double layer decreases while the total amount of anions in the electrical double layer increases when the adsorbate is present in the adsorbed phase [14]. Furthermore, the results in Fig. 2 show that the concentration, $C_{p2,ec}$, of the anions in the electroneutral core region of the pores also decreases from the center of the particle ($r/r_p=0$) to the surface of the particle ($r/r_p=\pm1$) because the anions move into the electrical double layer in order to facilitate the adsorption process of the analyte [14]. The results in Fig. 3 clearly indicate that a hump is present in the radial profile of the concentration, $C_{p3,ec}$, of the adsorbate in the electroneutral core region of the pores for times $t<t_5$ (for times t before the adsorption system comes to equilibrium). For times $t<t_5$, (i) the rate of transport of the cations from $r/r_p=0$ to $r/r_p=\pm1$ and the rate of transport of the adsorbate from the surface of the particle ($r/r_p=\pm1$) to the center of the particle ($r/r_p=0$) are significantly affected, through the condition of electroneutrality in the electroneutral core region of the pore fluid, by the rate of transport of the anions from the center ($r/r_p=0$) to the surface ($r/r_p=\pm1$) of the particle, (ii) the distribution of the concentrations of the adsorbate and of the cations in the electrical double layer and the concentration of the adsorbate in the adsorbed phase are controlled by the rate of transport of the anions to the adsorption zone (anions are needed in the adsorption zone to facilitate the adsorption process of the positively charged analyte for the reasons presented in Ref. [14]), (iii) the value of the concentration of the cations in the finite bath approaches the value of the concentration of the anions in the finite bath, through the condition of electroneutrality, as the adsorbate leaves the fluid of the finite bath and enters the particles, and this, in effect, creates a bottleneck for the transport of the adsorbate from the finite bath to the particles due to the relative differences in the mass transfer rates of the three different species (cation, anion, and adsorbate) through the liquid film (film mass transfer resistance) surrounding the particles, and this bottleneck in the transport of the adsorbate from the finite bath to the surface of the particles causes a significant decrease in the value of $C_{p3,ec}(t,\ r=r_p)$ with respect to time, and (iv) the bottleneck for the transport of the adsorbate at the particle surface ($r/r_p=\pm1$) induces a preponderance for the adsorbate in the concentration hump to move towards the center of the particle ($r/r_p=0$); the condition of electroneutrality restricts the transport of the adsorbate back to the surface of the particle ($r/r_p=\pm1$) because the difference in the values of $C_{p1,ec}$ and $C_{p2,ec}$ at the particle surface ($r/r_p=\pm1$) is

smaller than the difference in the values of $C_{p1,ec}$ and $C_{p2,ec}$ at inner radial positions in the particle. The effects of the mass transfer processes presented in items (i)–(iv) above, trap the adsorbate at some inner radial position in the particle leading to a hump in the radial profile of the concentration, $C_{p3,ec}$, of the adsorbate in the electroneutral core region of the fluid in the pores of the particles. The hump in the radial profile of $C_{p3,ec}$ leads, through Eqs. (5) and (6), to a hump in the radial profile of the concentration, C_{S3}, of the adsorbate in the adsorbed phase, as shown in Fig. 4; the hump in the radial profile of C_{S3} is considered to be the hump (concentration ring) observed in confocal scanning laser microscopy experiments.

The results in Figs. 5 and 6 indicate that there is a hump in the radial profiles of (a) the charge density, δ, on the surface of the pores, and (b) the electrostatic potential, Φ, evaluated at the surface ($\rho = \rho_{pore}$) of the pores. Furthermore, the results in Figs. 5 and 6 clearly show that the values of both δ and $\Phi(\rho = \rho_{pore})$ increase (become less negative) as the value of the concentration, C_{S3}, of the positively charged analyte in the adsorbed phase increases. The results in Fig. 7 show that the magnitude of the term $\exp[-(z_3 e/kT)\Phi(\rho = \rho_{pore})]$ is significantly larger than unity, and therefore, even if the value of the equilibrium adsorption constant, K, in Eq. (6) is not large, the product of K and $\exp[-(z_3 e/kT)\Phi(\rho = \rho_{pore})]$ can provide a number with a large positive magnitude which can provide a favorable adsorption isotherm.

It is important to mention here that the mathematical model presented in this work could be used to simulate adsorption systems of a single charged adsorbate having (i) values for the parameters of the model different than those employed in the adsorption simulations presented in this work, and (ii) adsorption isotherms whose expressions are different [1,2,26] than the expression (Eq. (6)) of the adsorption isotherm used in this work. Furthermore, the results presented here and results calculated from numerous simulations [15] using the mathematical model of this work, indicate that the relative magnitudes of the intraparticle diffusional mass fluxes of the cations, anions, and adsorbate influence significantly the magnitude and location of the humps in the concentrations of the adsorbate in the pore fluid ($C_{p3,ec}$) and in the adsorbed phase (C_{S3}). Thus, it is conceivable that, in single component adsorption systems where the effective pore diffusion coefficients of the cations, anions, and adsorbate change in magnitude with time and radial position in the particle due to (a) loading of the adsorbate in the adsorbed phase (restricted pore diffusion [12,20–22]), and (b) changes in the values of the concentrations of the cations, anions, and adsorbate in the pore fluid of the adsorbent particles, the analyte (adsorbate) could be trapped at more than one inner radial position in the particle leading to more than one hump in the radial profiles of the concentrations of the adsorbate in the pore fluid ($C_{p3,ec}$) and in the adsorbed phase (C_{S3}); these multiple humps could be considered to represent multiple concentration rings in the adsorbed phase of porous particles observed [9] by confocal scanning laser microscopy experiments. Finally, it should also be mentioned here that numerous simulations [15] using the mathematical model of this work have shown that humps (concentration rings) cannot develop for certain values of the parameters of the model that do not allow the interactions between the electrostatic potential distribution and the mechanisms of mass transport of the species by diffusion and adsorption to trap the adsorbate at an inner radial position in the particle; in such cases, the dynamic behavior of the analyte in the adsorbed phase exhibits a monotonic decrease in the value of its concentration from the surface to the center of the particle, as has also been observed in certain confocal scanning laser microscopy experiments [4–6].

4. Conclusions and remarks

A theoretical model for single component adsorption that accounts for the presence of an electrical double layer in the pores of adsorbent particles was constructed and solved. The dynamic behavior of the mechanisms of the model can result in the development of inner radial humps (concentration rings) in the concentration of a single charged analyte (adsorbate) in the adsorbed phase of porous charged adsorbent particles. The results of the present work demonstrate the implication of the concept regarding the effect of the presence of an electrical

double layer in the pores of adsorbent particles and the induced interactions between the electrostatic potential distribution and the mechanisms of mass transport of the species by diffusion, electrophoretic migration, and adsorption. Furthermore, the mechanisms of the model presented in this work could explain qualitatively the development of the concentration ring (hump) observed in confocal scanning laser microscopy experiments.

The theoretical model will be extended to also include the possible contribution of induced intraparticle electrophoretic migration due to the possible explicit variation of the electrostatic potential, Φ, along the radial direction, r, of the particles [13,14] as well as the possibility of having no electroneutral region anywhere in the pore fluid. The results that will be obtained from the extended theoretical model will be reported in the future.

5. Nomenclature

$C_{di}(t)$ Concentration of component i ($i=1, 2, 3$) in the fluid of the finite bath, mol/m^3

C^0_{d3} Concentration of analyte (adsorbate) in the fluid of the finite bath at time $t=0$, mol/m^3

$C_{pi}(t,r,\rho)$ Concentration of component i ($i=1, 2, 3$) in the pore fluid of the adsorbent particles (Eq. (7)), mol/m^3

$C_{pi,ec}(t,r)$ Concentration of component i ($i=1, 2, 3$) in the electroneutral core region of the pore fluid of the adsorbent particles, mol/m^3

$C_{pi}(t,r,\rho=\rho_{pore})$ Concentration of component i ($i=1, 2, 3$) in the liquid layer immediately adjacent to the surface of the pores of the adsorbent particles, mol/m^3

C_{S3} Concentration of analyte (adsorbate) in the adsorbed phase of the adsorbent particles, mol/m^3

C_T Maximum concentration of analyte (adsorbate) in the adsorbed phase of the adsorbent particles when all accessible adsorption sites are utilized, mol/m^3

$C_{+\infty}$ Concentration of the cations in the electroneutral core region of the pore fluid of the adsorbent particles at time $t=0$ when there is no analyte (adsorbate) present in the particles, mol/m^3

$C_{-\infty}$ Concentration of the anions in the electroneutral core region of the pore fluid of the adsorbent particles at time $t=0$ when there is no analyte (adsorbate) present in the particles, mol/m^3

$D_{mf,i}$ Free molecular diffusion coefficient of component i ($i=1, 2, 3$), m^2/s

D_{pij} Effective pore diffusion coefficient ($i=1, 2, 3$; $j=1, 2, 3$) in the pore fluid of the adsorbent particles, m^2/s

D_{pi} Effective pore diffusion coefficient of component i ($i=1, 2, 3$) in the pore fluid of the adsorbent particles [$D_{pi}=D_{pii}$ ($i=1, 2, 3$) where D_{pii} are the diagonal elements of the effective pore diffusivity matrix in Eqs. (8)–(10)], m^2/s

e Charge of one electron, C

K Equilibrium adsorption constant, mM^{-1}

K_{fi} Film mass transfer coefficient of component i ($i=1, 2, 3$), m/s

k Boltzmann constant, J/K

N_0 Avogadro's number, mol^{-1}

R_{di} Molar rate of production of species i ($i=1, 2, 3$) per unit volume of the finite bath, $mol/(m^3\ s)$

R_{pi} Molar rate of production of species i ($i=1, 2, 3$) per unit volume of the fluid in the pores of the adsorbent particles, $mol/(m^3\ s)$

r Radial coordinate of the adsorbent particles, m

r_p Radius of the spherical porous adsorbent particles in the finite bath, m

T Absolute temperature, K

t Time, s

z_i Charge number of component i ($i=1, 2, 3$), dimensionless

Greek letters

α	Form factor; 0, 1 and 2 for slab, cylinder and sphere, respectively, dimensionless
δ	Local charge density on the surface of the pores of the adsorbent particles, C/m^2
δ_0	Charge density on the surface of the pores of the adsorbent particles at $t=0$, C/m^2
ϵ	Dielectric constant of the liquid phase, dimensionless
ϵ_b	Void fraction in the finite bath, dimensionless
ϵ_0	Permittivity of free space, $C^2/(N\ m^2)$
ϵ_p	Porosity of the adsorbent particles, dimensionless
ρ	Radial coordinate of the pores in the adsorbent particles, m
ρ_{pore}	Average radius of the pores in the adsorbent particles, m
Φ	Electrostatic potential along the radius, ρ, of the pores of the adsorbent particles at time t and position r in the particle, J/C
$\Phi(\rho=\rho_{pore})$	Electrostatic potential at the surface of the pores of the adsorbent particles at time t and position r in the particle, J/C
ζ_w	Zeta potential at the surface of the pores in the adsorbent particles, J/C
ξ	Particle phase ratio, m^2/m^3

Subscripts

ec	Electroneutral core region
1	Cation
2	Anion
3	Positively charged analyte

Acknowledgements

Prof. A.I. Liapis and Mr. B.A. Grimes gratefully acknowledge support of this work by the University of Missouri Research Board and the Biochemical Processing Institute of the University of Missouri-Rolla.

References

[1] B.H. Arve, A.I. Liapis, AIChE J. 33 (1987) 179.
[2] A.I. Liapis, Sep. Purif. Methods 19 (1990) 133.
[3] A. Ljunglöf, J. Thömmes, J. Chromatogr. A 813 (1998) 387.
[4] H.-B. Kim, M. Hayashi, K. Nakatani, N. Kitamura, Anal. Chem. 68 (1996) 409.
[5] A. Ljunglöf, R. Hjorth, J. Chromatogr. A 743 (1996) 75.
[6] A. Ljunglöf, P. Bergvall, R. Bhikhabhai, R. Hjorth, J. Chromatogr. A 844 (1999) 129.
[7] A.M. Lenhoff, S.R. Dziennik, presented at the 1999 Annual Meeting of the American Institute of Chemical Engineers, Dallas, TX, 31 October–5 November 1999, paper 22b.
[8] A. Ljunglöf, T. Linden and J. Thömmes, presented at the 13th International Symposium on Preparative/Process Chromatography (PREP 2000), Washington, DC, 14–17 May 2000, paper L-303.
[9] S.R. Dziennik, A.M. Lenhoff, presented at the 13th International Symposium on Preparative/Process Chromatography (PREP 2000), Washington, DC, 14–17 May 2000, paper L-302.
[10] S.R. Dziennik, E.B. Belcher, A.M. Lenhoff, presented at the 20th International Symposium on the Separation and Analysis of Proteins, Peptides and Polynucleotides (ISPPP 2000), Ljubljana, Slovenia, 5–8 November 2000, paper L-102.
[11] G.A. Heeter, A.I. Liapis, J. Chromatogr. A 760 (1997) 55.
[12] J.J. Meyers, A.I. Liapis, J. Chromatogr. A 852 (1999) 3.
[13] B.A. Grimes, J.J. Meyers, A.I. Liapis, J. Chromatogr. A 890 (2000) 61.
[14] B.A. Grimes, A.I. Liapis, J. Colloid Interf. Sci. 234 (2001) 223.
[15] B.A. Grimes, Report No. 5, Department of Chemical Engineering, University of Missouri-Rolla, Rolla, MO, 2001.
[16] R.F. Probstein, Physicochemical Hydrodynamics, Wiley, New York, 1994.
[17] H.L. Toor, K.R. Arnold, Ind. Eng. Chem. Fundam. 4 (1965) 363.
[18] H.L. Toor, Intracellular Transport, Academic Press, New York, 1967.
[19] A.I. Liapis, R.J. Litchfield, Trans. IChemE 59 (1981) 122.
[20] J.H. Petropoulos, A.I. Liapis, N.P. Kolliopoulos, J.K. Petrou, N.K. Kanellopoulos, Bioseparation 1 (1990) 69.
[21] J.J. Meyers, O.K. Crosser, A.I. Liapis, J. Chromatogr. A 908 (2001) 35.
[22] J.J. Meyers, S. Nahar, D.K. Ludlow, A.I. Liapis, J. Chromatogr. A 907 (2001) 57.
[23] J. Villadsen, M.L. Michelsen, Solution of Differential Equation Models by Polynomial Approximation, Prentice-Hall, Englewood Cliffs, NJ, 1978.
[24] C.D. Holland, A.I. Liapis, Computer Methods for Solving Dynamic Separation Problems, McGraw-Hill, New York, 1983.
[25] C.J. Geankoplis, Transport Processes and Unit Operations, Allyn and Bacon, Boston, MA, 1983.
[26] A.I. Liapis, in: A.B. Mersmann, S.E. Scholl (Eds.), Fundamentals of Adsorption, Engineering Foundation (available from American Institute of Chemical Engineers), New York, 1991, p. 25.